Experimental report

15/12/2020

Proposal: **5-31-2685** **Council:** 4/2019

Title: Crystal and magnetic structures ofnovel Cr(II)-containing hybrid perovskites

Research area: Materials

This proposal is a new proposal

Main proposer: **Jose Antonio ALONSO**

Experimental team: Carmen ABIA SANZ
Jose Antonio ALONSO
Joao Elias RODRIGUES

Local contacts: Maria Teresa FERNANDEZ DIAZ

Samples: CsPbBr3
CrSiTe3
MAPb1-xCrx(Br,Cl)3, x= 0.25, 0.5
Co3AlSi3O12
Cs2AgSbCl6
P (black)

Instrument	Requested days	Allocated days	From	To
D2B	2	1	20/01/2020	21/01/2020
D20	2	2	18/09/2019	20/09/2019

Abstract:

Recently, theoretical calculations revealed the possibility of stabilizing Cr-substituted hybrid perovskites; the introduction of Cr(II) ions would not lead to an important cell distortion, while the energetic of the substitution process would induce new electronic states promoting an improved sunlight absorption. This prompted us to prepare Cr(II)-substituted samples in the series CH3NH3Pb1-xCrxBr3-2xCl2x (x= 0.25, 0.5). It is important to highlight that it is the first case of a perovskite framework containing Cr(II) ions. These ions are extremely unstable in solid state, since they are prone to oxidize to Cr3+. Cr(II) is a 3d4 ion, isoelectronic with Mn3+, and it is expected to induce Jahn-Teller-type distortions and interesting structural and magnetic features. The magnetic measurements show an overall antiferromagnetic behavior with a TN of 40 K, suggesting some canting of the Cr(II) magnetic moments. The aim of this proposal is to characterize and refine the crystal and magnetic structures of these two compounds in the 5-300 K range. The CH3NH3+ groups will certainly lose part of mobility and delocalization at low temperatures, due to orientational order-disorder phenomena.

Suitable optoelectronic properties have guided the interest in hybrid organic-inorganic perovskites in order to develop efficient photovoltaic devices. These compounds of general formula AMX_3 (A = organic cation, typically methyl-ammonium (CH_3NH_3): MA; B = metal; X= halogen) have attracted notable attention of the scientific community since the implementation of $CH_3NH_3PbI_3$ (also known as MAPI) in solar-cell heterojunctions resulted in efficiencies above 20 % [1, 2]. An adequate direct bandgap of ~1.6 eV of MAPI permits a broad absorption range over the complete visible light region, which goes along with high carrier mobility and long diffusion length of charge carriers [3]. The sensitivity to humidity is diminished with alternative halogens (X= Br, Cl) in the perovskite structure.

Recently, theoretical calculations by the density functional theory (DFT), as well as many-body perturbation methods along with spin-orbit coupling (SOC) revealed that partially Cr-substituted MAPI perovskites ($CH_3NH_3Pb_{1-x}Cr_xI_3$) are possible; the introduction of Cr^{2+} ions would not lead to an important cell distortion, while the energetic of the substitution process would induce new electronic states in the host semiconductor bandgap promoting an improved sunlight absorption [4].

These ab-initio calculations prompted us to prepare Cr^{2+}-substituted samples, which was realized in the series $CH_3NH_3Pb_{1-x}Cr_xBr_{3-2x}Cl_{2x}$ (x= 0.25, 0.5). They were obtained by mechano-synthesis in a planetary ball mill from MABr, $PbBr_2$ and $CrCl_2$, working in Ar atmosphere. The XRD patterns can be refined in a cubic *Pm-3m* unit cell. It is important to highlight that it is the first case of a **perovskite framework containing Cr^{2+} ions**. These ions are **extremely unstable** in solid state, since they are prone to oxidize to Cr^{3+}. Cr^{2+} is a $3d^4$ ion, isoelectronic with Mn^{3+}, and it is expected to induce Jahn-Teller-type distortions and interesting structural and magnetic features.

Two samples were thus prepared and filled into 6 mm vanadium holders, sealed under inert N_2 atmosphere; $MAPb_{0.5}Cr_{0.5}Br_{2.5}Cl_{0.5}$ and $MAPb_{0.75}Cr_{0.25}Br_{2.75}Cl_{0.25}$.

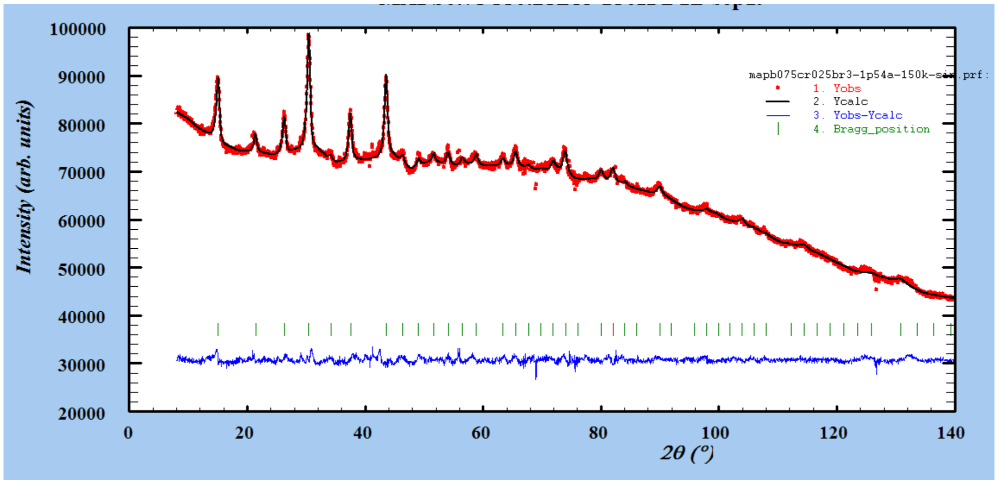

Figure 1. *Le-Bail fit of a NPD pattern collected for $MAPb_{0.75}Cr_{0.25}Br_{2.75}Cl_{0.25}$ at D20, with λ= 1.54 Å and 90° as take-off angle. All the reflections can be indexed in a cubic pattern with a= 5.8654(9) Å, at 150 K.*

Despite the precautions taken to avoid the decomposition of the very unstable samples, the acquired diffraction diagrams, either at D2B or D20, were of poor quality, with high background levels and weak reflection intensity; an example for x= 0.25 is shown in Figure 1, collected at D20 with λ= 1.54 Å and 90º as take-off angle. The plot shows a pattern matching of the profile at 150 K, corresponding to a cubic structure with a= 5.8654(9) Å. The treatment of the structural features of this compound is in progress.

Given the mediocre acquisitions of the Cr-containing samples, part of the allotted time was devoted to complete a structural study of the compound $CsPbBr_3$, for which a previous preliminary investigation was carried out from synchrotron x-ray powder diffraction [5]. A complete temperature dependent sequential collection was acquired at D20, from 4 K to 100 K, with a wavelength of 1.540 Å. The sample, contained in a V cylinder, was introduced in a standard “orange” cryostat and measured at 100 K for 1 h, and then cooled down to 4 K while acquiring sequential patterns every 3 min. Finally, a good statistics pattern was collected at 4 K for 30 min.

$CsPbBr_3$ is orthorhombic at RT, with a classical *Pbnm* superstructure due to the tilting of the $PbBr_6$ octahedra. Fig. 2 shows the refined SXRD pattern at RT, including a view of the crystal structure.

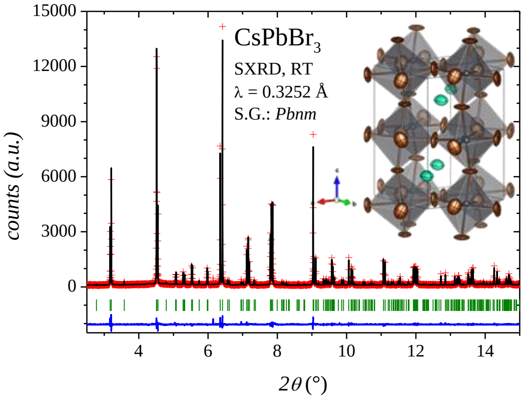

Figure 2. *Observed (crosses) calculated (black line) and difference (blue line) profiles after the Rietveld refinement in an orthorhombic cubic unit cell from SXRD data. Inset: View of the crystal structure enhancing the tilting of the* $PbBr_6$ *octahedra and the anisotropic displacement factors.*

D20 NPD data show that the orthorhombic unit-cell is maintained down to 4 K. Figure 3 shows the *a*, *b* and *c* unit-cell parameters variation as well as the Rietveld plot at 4 K. It is remarkable that *a* and *c* parameters decrease, whereas b increases upon cooling. This conspicuous effect of negative thermal expansion along the *b* axis had not been reported before in $CsPbBr_3$. Normally, negative thermal expansion in *Pbnm* perovskites is a consequence of magnetostricive effects, concomitant with magnetic ordering, for instance in rare-earth ferrites. In $CsPbBr_3$, it deserves further analysis. The octahedral tiltings at 4 K are 10.97° and 14.11° for anti-phase and in-phase tilts, respectively. The thermal evolution (including the RT and the range between 100 and 4 K) of the tilts shows a linear behavior for both phase and anti-phase octahedral rotations.

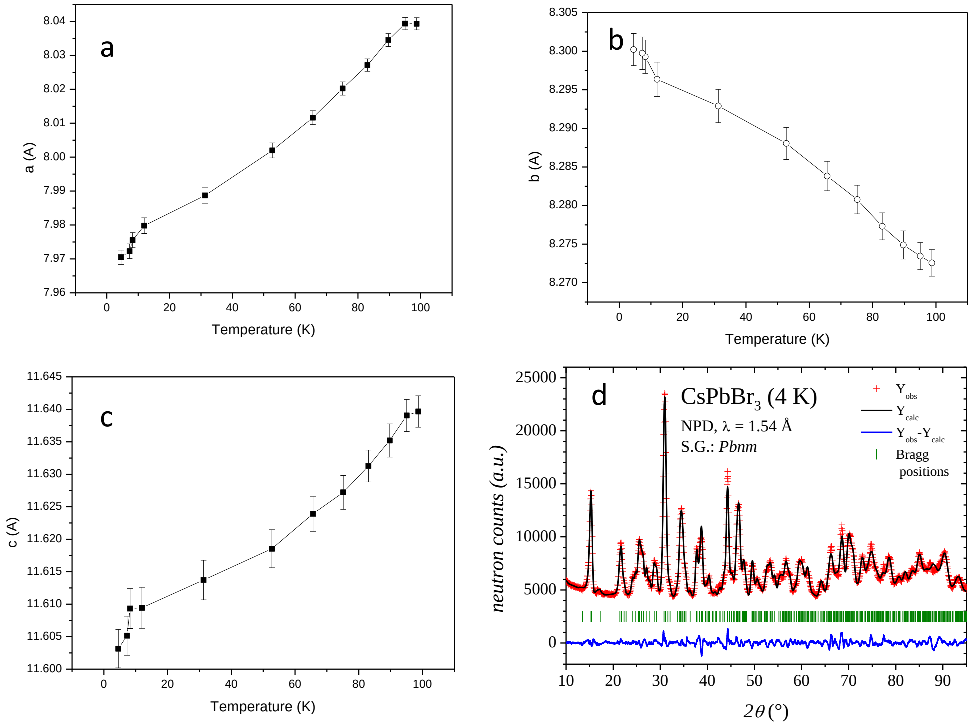

Figure 3. (a) a, (b) b and (c) c unit-cell parameters thermal evolution from D20 NPD data; (d) Rietveld NPD profiles at 4 K.

This work has been published in ACS Omega in REF [5].

REFERENCES

1. Park N-G (2015). Mater Today 18:65–72.
2. Liu M, Johnston MB, Snaith HJ (2013). Nature 501:395.
3. Wehrenfennig C, Eperon GE, Johnston MB, et al. (2014) Adv Mater 26:1584–1589.
4. García G, Palacios P, Menéndez-Proupin E, et al. (2018) Sci Rep 8:2511.
5. C. A. López, C. Abia, M.C. Alvarez-Galván, B.K. Hong, M. V. Martínez-Huerta, F. Serrano-Sánchez, F. Carrascoso, A. Castellanos-Gómez, M. T. Fernańdez-Díaz, and J. A. Alonso, ACS Omega 2020, 5, 5931−5938